X-RAY ANALYSIS OF THE CIS FORM OF 2.5 DIMETHYLTHIACYCLOPENTANE

by

GEORGE RAY GALLAGHER

A. B., Kansas State Teachers College, Emporia, 1953

A THESIS

submitted in partial fulfillment of the

requirements for the degree

MASTER OF SCIENCE

Department of Physics

KANSAS STATE COLLEGE
OF AGRICULTURE AND APPLIED SCIENCE

1955

TABLE OF CONTENTS

INTRODUCTION

The cis and trans forms of 2,5 Dimethylthiacyclopentane are mercuric chloride complexes of the cyclic sulfides. These derivatives are prepared by adding 0.025 mole of the cyclic sulfide to 0.125 mole mercuric chloride dissolved in 100 milliliters of ethanol. The solution is agitated for 30 minutes then cooled and filtered. The solid derivatives are then crystallized to a constant melting point from ethanol (Whitehead, et al, 8).

The cis form contains two mercuric chloride groups both presumed to be positioned on the same side of the ring, whereas the trans isomer includes only one mercuric chloride group. The cis and trans forms differ in space relationships within the molecule, and can occur in ring compounds where rigidity of ring structure prevents rotation.

The study presented here attempts to acquire knowledge of the crystal structure and the positions occupied by the mercury atoms in the cis form of the 2,5 Dimethylthiacyclopentane molecule. The x-ray diffraction method was the means chosen to attack the problem.

The x-ray unit used was a General Electric XRD-1 power supply utilizing a copper target tube. A nickel filter produced nearly monochromatic CuK_{α} radiation of average wavelength of 1.5418 A°.

A Weissenberg camera which operates on the moving film principle was used to obtain all photographs (Buerger, 2). The constants of the camera includes a calibrated diameter of 57.23 ± 0.04 millimeters and a synchronized film translation and crystal rotation of 90 millimeters and 180 degrees, respectively.

Since direct physical measurements of the photographs were necessary to carry out the analysis, as many individual measurements as possible were taken of each parameter in order to obtain a good statistical average.

PROCEDURE

Due to the crystal's high vapor pressure, it was necessary to coat it with collodion. The coating served the two fold purpose of supporting the fragment on the carbon mount and preventing it from vaporizing.

The crystal was aligned so that one of its axes was parallel to the rotation axis of the camera, and thereby perpendicular to the x-ray beam, by using the method outlined by Dragsdorf (4). It was found, however, that an exposure time of 20 minutes gave clearer patterns than the suggested time of from one to five minutes. After the proper alignment of the crystal was attained, a rotation photograph was made by allowing the crystal to rotate at a uniform angular velocity about the axis set perpendicular to the incident x-ray beam.

When x-rays strike a single plane of atoms at any glancing angle, θ, they are diffracted in such a way as to obey the standard laws of optical reflections. The condition that the reflections from each of the planes of atoms do not annul one another is that their individual reflected waves be in phase.

This condition is satisfied when reflection occurs at the Bragg angle given by Bragg's law,

$$\sin\theta = \frac{n\lambda}{2d}, \text{ where}$$

n = a positive integer

λ = wavelength

d = the distance between crystal planes.

If the rotation axis of the crystal is designated as the a_3 axis, then by Laue's equation (Bunn, 3),

$$(S - S_o) \cdot a_3 = \ell\lambda$$

where S = the unit vector giving the direction of the diffracted beam

S_o = the unit vector giving the direction of the incident beam

ℓ = an integer.

This becomes $S \cdot a_3 - S_o \cdot a_3 = \ell\lambda$, but $S_o \cdot a_3 = 0$ since S_o is perpendicular to a_3. Therefore, $|S| a_3 \cos(90-\beta) = \ell\lambda$ (See Plate I)

$$a_3 \sin\beta = \ell\lambda$$

$$\sin\beta = \frac{\ell\lambda}{a_3}$$

For a particular value of ℓ, β is constant, therefore, the diffracted rays appear to form two cones, one on each side of the incident beam, whose axis is parallel to the rotation axis. The second order diffractions form a narrower cone than the first order, the third order narrower than the second, etc. (Plate II). By using a cylindrical film, whose axis is the axis of rotation of the crystal, to record the x-ray pattern, the conical surface containing the diffracted beams will intercept the film in a series of parallel layer lines, Plate II.

The rotation pattern yields the necessary information for the setting of the layer line screen. This screen allows only reflections from the desired layer line to reach the film; all other reflections being absorbed by the screen. Proper setting of the screen made it possible to obtain Weissenberg photographs of the zero, one, and two layer lines.

EXPLANATION OF PLATE I

A section of cylindrical film, whose axis is parallel to the rotation axis of the crystal, showing the coordinates necessary to define a diffraction spot on a Weissenberg photograph.

PLATE I

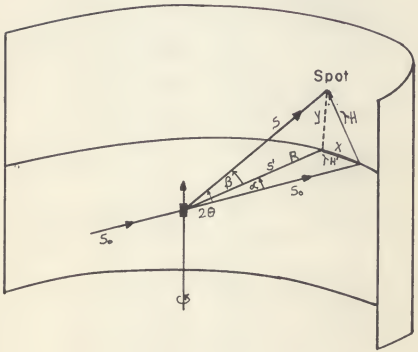

EXPLANATION OF PLATE II

Cones of diffraction intersecting a coaxial cylindrical film.

PLATE II

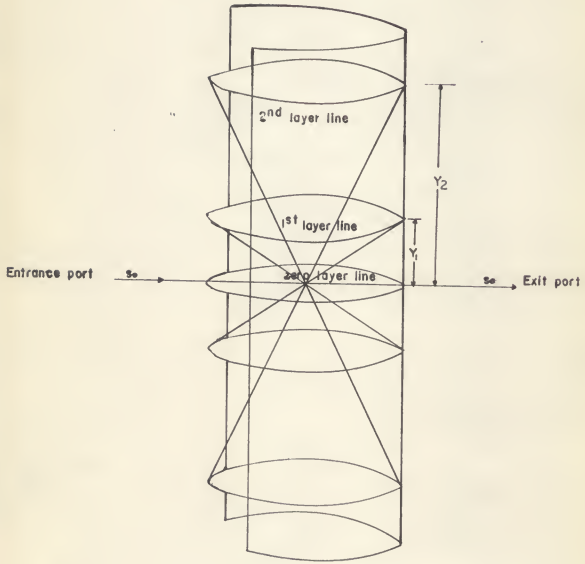
2nd layer line
Y2
1st layer line
Y1
Entrance port
So
Zero layer line
So
Exit port

Each spot on the Weissenberg photograph has two film coordinates, x and y, whereas the rotation photograph has only one coordinate, x. The layer line of a rotation photograph is thus the collapsed equivalent of a Weissenberg photograph in which the y coordinate has been eliminated. Another way of expressing this is that a Weissenberg photograph is the resolved equivalent of a layer line on a rotation pattern, where the resolved element is the y coordinate of each diffraction spot (Plate III).

Each of the various layer lines were exposed for 60 hours which assured maximum darkening of the strongest spots. A double film was used so that the relative intensities of the stronger spots could be differentiated. The information necessary for the construction of the reciprocal lattice may be obtained by direct measurement of the layer line photograph. Theoretically, the reciprocal lattice points are the tips of the H vectors. The H vectors define specific planes of the real lattice. These vectors are constructed perpendicular to the planes and are of magnitude equal to the reciprocal of the d spacing of the particular defined plane. Drawing all the H vectors for a given crystal lattice from an arbitrary origin and denoting only the tips of the vectors produces the reciprocal lattice.

The film to be interpreted was taped on an illuminated viewing stand, and a steel rule adjusted to its center. A celluloid triangle was then placed on the steel rule and shifted making each reflection successively coincide with the hypotenuse (Plate IV). The λH value for the spot was read from the vertical scale and the $\phi/2$ coordinate from the index on the base of the triangle, (Table 1). Plotting the angle ϕ and the corresponding λH values on polar coordinate paper gave the reciprocal lattice plot (Plate V).

The slope of the measuring triangle and its vertical calibration was determined from the following derivation.

EXPLANATION OF PLATE III

Fig. 1. A Weissenberg photograph showing a diffraction spot and its x and y components.

Fig. 2. A rotation photograph of the same spot recorded in Fig. 1, but having only one coordinate.

PLATE III

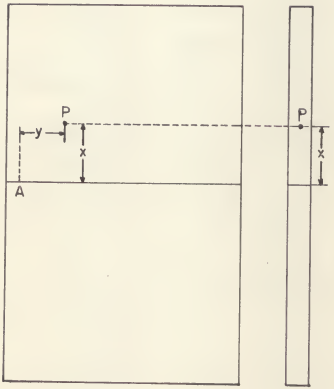

Fig. 1

Fig. 2

EXPLANATION OF PLATE IV

The calibrated triangle used for measuring the λH value and the $\phi/2$ coordinate for each diffraction spot on a Weissenberg photograph of the zero layer line.

PLATE IV

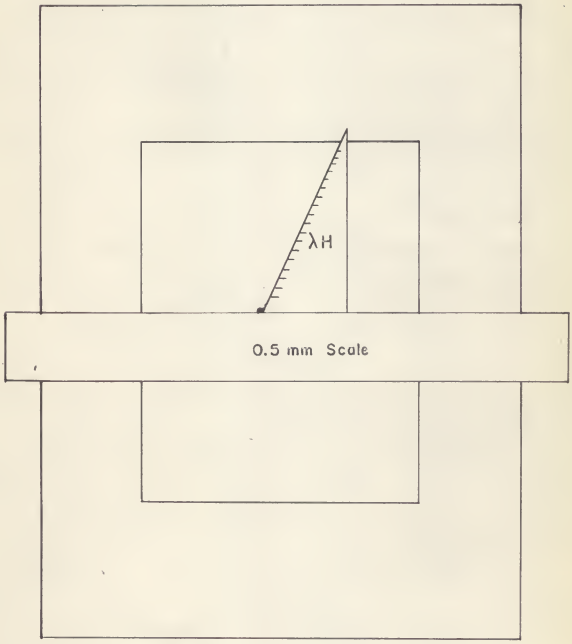

EXPLANATION OF PLATE V

A reproduction of the $\ell = 0$ reciprocal lattice.

PLATE V

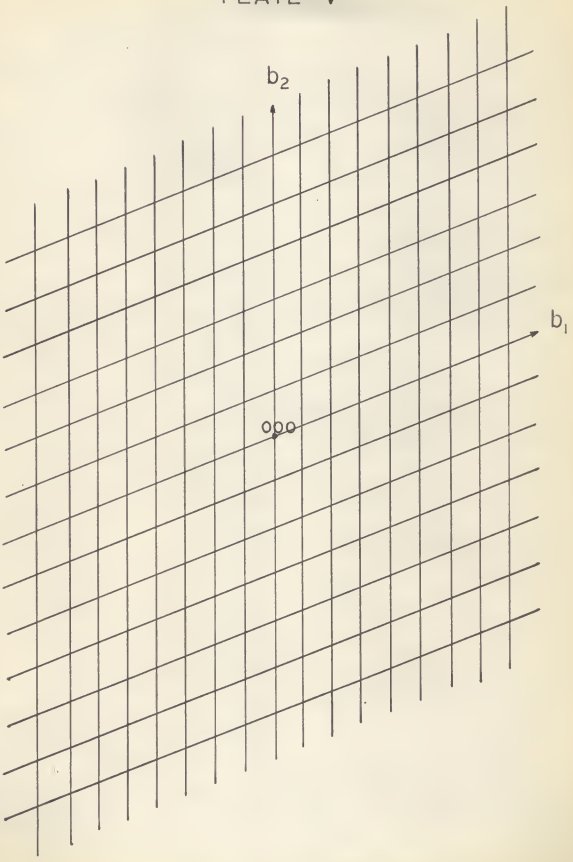

Table 1. Data obtained from the $\ell = 0$ Weissenberg photograph, the intensity calibration strip, and the θ vs. L.P. graph.

Line No.	λH	hkl	I(rel.)	θ	L.P.	F^2(rel.)
1	0.37	020	250	11.2	4.8	52
2	0.56	030	9	17.1	3.0	3
3	0.54	$1\bar{3}0$	250	16.0	3.2	78
4	0.89	$\bar{2}50$	50	26.9	1.6	31
5	0.35	$1\bar{2}0$	448	10.4	5.2	86
6	0.71	$\bar{2}40$	15	21.3	2.25	7
7	1.25	$1\bar{7}0$	10	39.3	1.0	10
8	0.89	$\bar{3}50$	10	26.9	1.6	6
9	0.53	$\bar{2}30$	60	15.7	3.3	18
10	0.72	$\bar{3}40$	30	21.5	2.21	14
11	0.36	$\bar{2}20$	374	11.0	4.9	76
12	0.75	$1\bar{4}0$	10	22.6	2.1	5
13	1.14	$\bar{6}60$	5	35.3	1.13	4
14	0.60	$\bar{3}30$	4	18.0	2.78	1
15	0.99	$\bar{6}50$	10	30.0	1.4	7
16	0.61	$1\bar{3}0$	25	18.3	2.8	9
17	0.80	$\bar{5}40$	4	24.0	1.92	2
18	1.05	$\bar{7}50$	30	32.2	1.25	24
19	0.43	$\bar{3}20$	70	12.8	4.12	17
20	1.14	$\bar{6}50$	20	35.0	1.18	17
21	0.69	$\bar{5}30$	55	20.5	2.4	23
22	1.23	$\bar{9}50$	8	38.7	1.03	8
23	0.52	$1\bar{2}0$	20	15.4	3.4	6
24	0.78	$\bar{6}30$	123	23.5	2.0	62
25	0.25	$\bar{2}10$	7	7.8	7.17	1
26	1.32	$10\bar{5}0$	4	41.7	1.0	4
27	0.89	$\bar{7}30$	42	26.9	1.61	26
28	0.63	$\bar{5}20$	6	18.8	2.65	2
29	0.99	$\bar{6}30$	9	30.1	1.4	6
30	0.36	$\bar{3}10$	55	11.0	4.88	11
31	0.74	$\bar{6}20$	5	22.0	2.19	2
32	0.86	$\bar{7}20$	6	26.0	1.72	3
33	1.35	$11\bar{3}0$	5	43.0	1.01	5

Table 1. Cont.

Line No.	λH	hkl	I(rel.)	θ	L.P.	F^2(rel.)
34	0.49	$\bar{4}10$	55	14.6	3.6	15
35	1.49	$\bar{1}230$	7	48.6	1.0	7
36	0.61	$\bar{5}10$	50	18.3	2.8	18
37	0.74	$\bar{6}10$	35	22.0	2.0	16
38	1.25	$\bar{1}0\bar{1}0$	5	39.3	1.01	5
39	1.40	$\bar{1}\bar{1}10$	5	45.0	1.0	5
40	0.25	$\bar{2}00$	144	7.8	7.17	20
41	0.38	$\bar{3}00$	67	11.5	4.62	15
42	0.51	$\bar{4}00$	13	15.4	3.39	4
43	0.65	$\bar{5}00$	52	19.3	2.59	20
44	0.79	$\bar{6}00$	50	23.6	1.98	25.3
45	0.92	$\bar{7}00$	19	28.0	1.57	12
46	1.05	$\bar{8}00$	16	32.2	1.27	8
47	1.19	$\bar{9}00$	4	37.0	1.09	4
48	1.46	$\bar{1}200$	4	47.8	1.0	4
49	1.15	$\bar{8}10$	6	35.5	1.15	5
50	1.00	$\bar{7}10$	4	30.1	1.4	3
51	1.13	$\bar{7}20$	7	34.9	1.2	6
52	1.00	$\bar{6}20$	11	30.1	1.4	11
53	0.87	$\bar{5}20$	27	26.3	1.68	16
54	0.75	$\bar{4}20$	42	22.6	2.09	20
55	0.64	$\bar{3}20$	29	19.0	2.61	11
56	0.98	$\bar{4}30$	6	29.9	1.41	4
57	0.25	$\bar{1}10$	28	7.8	7.18	4
58	0.53	$\bar{2}20$	5	15.9	3.25	2
59	0.80	$\bar{3}30$	5	24.0	1.93	3
60	1.08	$\bar{4}40$	5	33.3	1.21	4
61	0.98	$\bar{3}40$	17	29.9	1.41	12
62	0.70	$\bar{2}30$	26	21	2.30	11
63	0.90	$\bar{2}40$	15	27.2	1.60	10
64	1.30	$\bar{3}60$	5	41.0	1.01	5
65	0.63	$\bar{1}30$	43	18.7	2.70	16
66	0.82	$\bar{1}40$	11	24.8	1.83	6

Table 1. Concl.

Line No.	λH	hkl	I(rel.)	θ	L.P.	F^2(rel.)
67	1.01	$\bar{1}50$	5	34.0	1.20	4
68	0.37	$0\bar{2}0$	295	11.0	4.88	61
69	0.57	$0\bar{3}0$	400	17.2	2.95	136
70	0.95	$0\bar{5}0$	14	29.0	1.48	9
71	0.92	$1\bar{5}0$	41	27.8	1.59	26
72	1.27	$2\bar{7}0$	8	39.9	1.02	8
73	0.54	$1\bar{3}0$	500	16.0	3.23	155
74	0.90	$2\bar{5}0$	50	27.2	1.62	31
75	1.26	$3\bar{7}0$	13	39.7	1.02	13
76	0.71	$2\bar{1}0$	29	21.2	2.28	13
77	1.25	$4\bar{7}0$	6	39.3	1.03	6
78	1.51	$8\bar{8}0$	4	49.8	1.01	4

Plate VI shows a reciprocal lattice and its sphere of reflection (2, 7). The sphere was arbitrarily drawn through the origin O, with its center on the incident ray AO at a distance $|So|$, which is the radius of the sphere. The sphere is called "sphere of reflection" because reciprocal lattice points such as P will diffract the primary beam only when they lie on its surface (2,6,7). If the crystal is rotated, the sphere of reflection will sweep about the origin generating a torus in reciprocal lattice space. Reflections will occur whenever a lattice point touches the surface of the sphere. Laue's general equation states: $S-S_o = \lambda H$, where H = vector which specifies crystal planes

$$H = \frac{1}{d} = hb_1 + kb_2 + lb_3$$

d = distance between crystal planes.

Let the crystal rotate through an angle ψ until a reflection point P, is reached, (Plate VI). Thus:

$$\psi = \theta + \phi \qquad (1)$$

EXPLANATION OF PLATE VI

The $\ell = 0$ reciprocal lattice showing two positions of the sphere of reflections.

PLATE VI

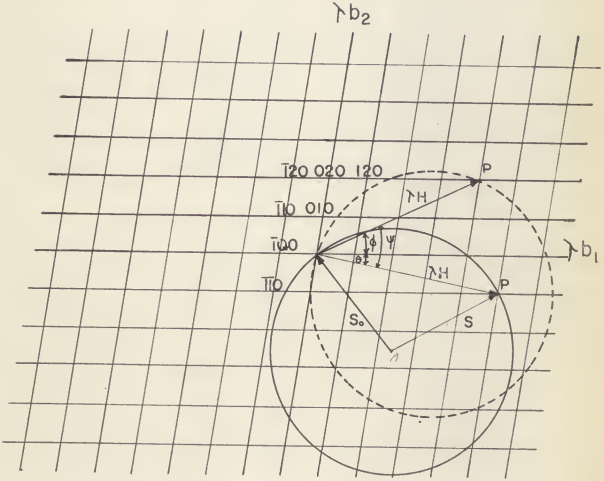

In the Weissenberg camera the crystal rotates 180° while the film translates 90 mm. This gives the ratio:

$$\frac{\psi^\circ}{180^\circ} = \frac{y}{90\ \text{mm}}.$$

$$\psi^\circ = 2\ y\ (\text{mm}) \tag{2}$$

where y is the distance in millimeters from an arbitrary point to the diffraction spot shown in Plate III.

Substituting equation (2) into equation (1)

$$2\ y\ (\text{mm}) = \theta^\circ + \phi^\circ \tag{3}$$

From Plate VII, Fig. 2,

$$2\theta R = x\ (\text{mm})$$

$$\theta = \frac{x(\text{mm})}{2R(\text{mm})} \qquad \text{where } \theta \text{ is in radians}$$

$$\theta^\circ = \frac{x(\text{mm})}{\frac{180}{\pi}\ (\text{mm})}\ \frac{180}{\pi}$$

$$\theta^\circ = x(\text{mm})$$

Substituting this value back into equation (3) gives,

$$2\ y\ (\text{mm}) = x\ (\text{mm}) + \phi^\circ.$$

Taking the derivative to find the slope,

$$\Delta y = \frac{\Delta x}{2}$$

$$\frac{\Delta y}{\Delta x} = 1/2$$

Therefore, for the equatorial layer line the triangle will have a slope of 1/2, corresponding to an angle of 63° 26' with the horizontal. From Plate IV it is seen that the x coordinate is always zero since measurements are taken at the bottom of the triangle. Substituting this value of x in equation 3, gives the relation between y and ϕ.

$$2y = 0 + \phi^{\circ}$$
$$2y\ (mm) = \phi^{\circ} \qquad (4)$$

The y coordinate can be read directly from the film and its value doubled for ϕ. From Laue's general equation:

$$|S-S_o| = |\lambda H|$$
$$|S-S_o| = 2 \sin\theta = |\lambda H|$$

but $\theta^{\circ} = x\ (mm)$,

therefore, $2 \sin x\ (mm) = |\lambda H|$

$$x\ (mm) = \sin^{-1}\ (\frac{\lambda H}{2}) \qquad (5)$$

Since the sine cannot exceed the value unity, λH is restricted to values of from zero to two.

By letting λH assume values from zero to two in steps of .05, equation 5 will give corresponding values of x. This allows the hypotenuse of the triangle to be calibrated directly in terms of λH.

The $\ell = n\ (n \neq o)$ layer lines presents a somewhat different approach since they are situated in layers above the $\ell = 0$ lattice. This makes it necessary to use the horizontal components of some of the vectors in the calibration derivation. The result is that the measuring triangle will not have a constant slope.

The heavy lines in Plate VIII represents the $\ell = 0$ reciprocal lattice and the dotted lines the $\ell = n\ (n \neq o)$ lattice, which is postioned some distance above the $\ell = 0$ lattice.

If ψ is the angle of rotation of the crystal, then $\psi = \eta + \phi$. η and ϕ are the respective angles between the b_1 axis and the H vector before and after rotation,

$$\frac{\psi}{180^\circ} = \frac{y\ (mm)}{90\ (mm)}$$

$$\psi' = 2\ y\ (mm)$$

From the rotation photograph, Plate I,

$$\tan \beta = y/R$$

$$\beta = \tan^{-1}\ (y/R)$$

Plate VII, Fig. 1 gives $S'/\lambda = S/\lambda \cos\beta$.

By the cosine law,

$$H'^2 = \left(\frac{S_o}{\lambda^2}\right)^2 + \left(\frac{S'}{\lambda^2}\right)^2 - 2\,\frac{S_o}{\lambda}\,\frac{S'}{\lambda}\cos\alpha.$$

But $S'/\lambda = S\cos\beta$ and $|S_o| = |S| = 1$

so $$H'^2 = \frac{1}{\lambda^2} + \frac{\cos^2\beta}{\lambda^2} - 2\cos\beta\,\frac{\cos\alpha}{\lambda^2} \qquad (6)$$

$$\lambda H' = (1 + \cos^2\beta - 2\cos\beta\cos\alpha)^{1/2}$$

From Plate II,

$$\alpha R\ (mm) = x\ (mm)$$

$$\alpha = \frac{x(mm)}{R(mm)} = \frac{2\ x\ (mm)}{2R(mm)} \qquad \left\{\begin{array}{l}\text{where } \alpha \text{ is in}\\ \text{radians}\end{array}\right.$$

$$\alpha^\circ = \frac{2\ x\ (mm)}{180\ (mm)}\ \frac{180}{\pi}$$

$$\alpha^\circ = 2\ x\ (mm)$$

This relation substituted into equation (6) gives,

$$\lambda H' = \left[1 + \cos^2\beta - 2\cos\beta\cos 2\ x\ (mm)\right]^{\frac{1}{2}}$$

$$\cos 2\ x\ (mm) = \frac{1 + \cos^2\beta - \lambda^2 H'^2}{2\cos\beta}$$

$$2\ x\ (mm) = \cos^{-1}\left(\frac{1 + \cos^2\beta - \lambda^2 H'^2}{2\cos\beta}\right) \qquad (7)$$

β is a constant for a particular layer line so by allowing $\lambda H'$ to assume values from zero to two in steps of .05, corresponding values of x are

EXPLANATION OF PLATE VII

Fig. 1. Enlarged view of the base of the spherical triangle of Plate I.

Fig. 2. A cross sectional view of the cylindrical film looking along the axis of the camera.

PLATE VII

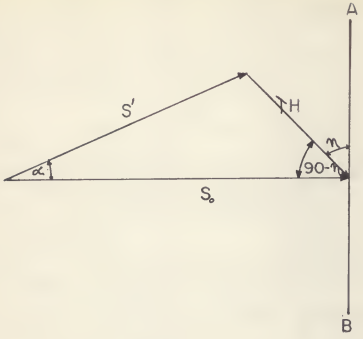

Fig. 1

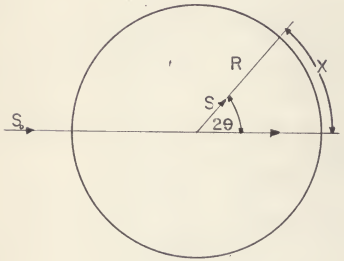

Fig. 2

EXPLANATION OF PLATE VIII

The $\ell = 1$, dotted lines, reciprocal lattice superimposed upon the $\ell = 0$, solid lines, reciprocal lattice.

PLATE VIII

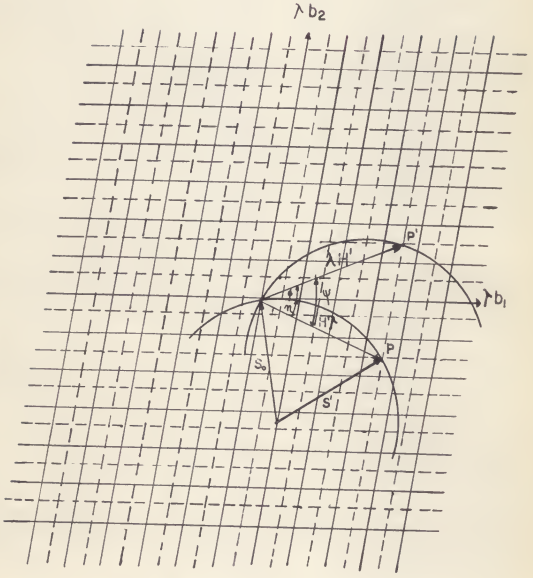

obtained. Plate VII, Fig. 1 is a reproduction of the base of the spherical triangle illustrated in Plate I. AD is perpendicular to S_o/λ and corresponds to the b_1 axis of the reciprocal lattice.

By the law of sines:

$$\frac{\sin(90-\eta)}{S'/\lambda} = \frac{\sin\alpha}{H'}$$

$\sin(90-\eta) = \cos\eta$ and $S'/\lambda = S/\lambda \cos\beta$, therefore:

$$\frac{\cos\eta}{S\cos\beta} = \frac{\sin\alpha}{\lambda H'}$$

and

$$\cos\eta = \frac{\sin\alpha \cos\beta}{\lambda H'}$$

$$\eta = \cos^{-1}\left(\frac{\sin\alpha \cos\beta}{\lambda H'}\right)$$

$$\eta = \cos^{-1}\left(\frac{\sin 2x \cos\beta}{(1 \cos^2\beta - 2\cos\beta \cos 2x)^{\frac{1}{2}}}\right)$$

since $\lambda H' = (1 + \cos^2\beta - 2\cos\beta\cos\alpha)^{\frac{1}{2}}$ and $\alpha = 2x$ (mm).

But $\psi^\circ = \eta^\circ + \phi^\circ$

therefore $\psi^\circ = 2y = \cos^{-1}\left(\frac{\sin 2x \cos\beta}{(1 + \cos^2\beta - 2\cos\beta\cos 2x)^{\frac{1}{2}}}\right) + \phi^\circ$

Substituting in the values of x found from equation 7 corresponding values of y were calculated. Plotting x vs y on millimeter graph paper gave the desired shape of the measuring device.

When measuring the film, x = o. Therefore,

$$\psi^\circ = 2y = \cos^{-1}(0) + \phi^\circ$$

$$2y = 90^\circ + \phi^\circ$$

Since y is measured from an arbitrary point, the correction term may be neglected and $2y(mm) = \phi^\circ$.

The relative intensities of the diffraction spots must be known in order to compute the relative crystal structure factors, F(hkl). The intensity

of a diffracted x-ray beam at a point p is, $I_p = \frac{I_o e^4}{m^2 c^4 R^2} \left(\frac{1 + \cos^2 2\theta}{2 \sin 2\theta} \right)$ $F(hkl)^2$ (2), where,

I_p = Intensity of beam at point P

I_o = intensity of incident beam

e = charge of an electron

m = mass of electron

c = velocity of light

R = distance from diffraction center to point P

$\frac{(1 + \cos^2 2\theta)}{2 \sin 2\theta}$ = Lorentz polarization term, (L.P.)

F(hkl) = Crystal structure factor

This may be written as $I_p = K \left(\frac{1 + \cos^2 2\theta}{\sin 2\theta} \right) F(hkl)^2$ where $K = \frac{I_o e^4}{2m^2 c^4 R^2}$ and is a constant. Since only the relative intensities are desired, the equation may be written as;

$$I_p \propto (L.P.)\, F(hkl)^2.$$

The crystal was rotated until a strong diffraction plane was in a reflecting position. Exposures were made of this diffraction spot for times ranging from two and one-half to zero minutes dropping in steps of one-half of one second for each exposure. The film was translated after each exposure, thus giving a strip containing 300 spots ranging in intensity from zero to maximum blackening. The calibrated strip was then used to determine the relative intensity of each diffraction spot of the equatorial layer line. A graph of θ versus the Lorentz-Polarization factor was plotted for values of θ ranging from zero to 90° and Lorentz-Polarization terms from $-\infty$ to $+\infty$. The angle θ $[\theta^\circ = x(mm)]$ for each diffraction spot was measured

and from the graph its Lorentz-Polarization factor determined. Using the relation $I \propto (L.P.)\, F(hkl)^2$, the relative $F(hkl)^2$ value for each diffraction spot was calculated.

The Patterson analysis gives a method of obtaining information about interatomic distances in crystals by using a Fourier series, the coefficients of which are the values of $F(hkl)^2$ instead of those of $F(hkl)$. This procedure is very useful due to the fact that it does not take account of the relative phases of the reflections and requires no assumptions based on tentative ideas of the structure of the crystal.

The crystal structure factor, $F(hkl)$ is given by:

$$F(hkl) = \sum_n f_n \exp\ 2\pi i(hx+ky+\ell z)$$

where, f_n = atomic scattering factor of the n^{th} atom

x,y,z = fractional increments along a_1, a_2, a_3, respectively, for the position of the n^{th} atom.

This may be written more generally for an electron distribution as,

$$F(hkl) = \int_V \rho(x,y,z)\, dV\ e^{2\pi i(hx+ky+\ell z)}$$

$$F(hkl) = \int_0^{1'}\int_0^{1'}\int_0^{1'} \rho(x,y,z)\, V\, e^{2\pi i\,(hx+ky+\ell z)}\, dx\, dy dz$$

and finally

$$F(hkl) = V \int_0^{1'}\int_0^{1'}\int_0^{1'} \rho(x,y,z)\, e^{2\pi i(hx+ky+\ell z)}\, dxdydz$$

The Fourier series representation of the electron density at a point (x,y,z) in a crystal is,

$$\rho(x,y,z) = \frac{1}{V} \sum_{h'} \sum_{k'=-\infty}^{+\infty} \sum_{\ell'} F(h'k'l')\, e^{-2\pi i(h'x+k'y+\ell' z)}$$

Consider the function $\rho(x+u,\ y+v,\ z+w)$, where u, v, and w are parameters kept constant while x, y, z vary. The function $\rho(x+u,\ y+v,\ z+w)$ represents an

electron density exactly similar to that corresponding to $\rho(x,y,z)$, but displaced with reference to it. The product of the two integrated over all of the cell is the Patterson function, P.

$$P(u,v,w) = \int_0^1\int_0^1\int_0^1 \rho(x,y,z)\ \rho(x+u,\ y+v,\ z+w)\ dx\ dy\ dz$$

Substituting in the density representations gives:

$$P(u,v,w) = \frac{1}{V^2}\int_0^1\int_0^1\int_0^1 \sum_h\sum_k\sum_l \sum_{h'=-\infty}^{+\infty}\sum_{k'}\sum_{l'} F(hkl)\exp.\left[-2\pi i(hx+ky+lz)\right] F(h'k'l')\exp.$$
$$\left[-2\pi i\{h'(x+u)+k'(y+v)+l'(z+w)\}\right]$$

The integral vanishes unless $h=-h'$, $k=-k'$, $l=-l'$. In this case $F(hkl) = F^*(h'k'l')$, and $P(u,v,w) = \frac{1}{V^2}\sum_h\sum_k\sum_{l=-\infty}^{+\infty} F(hkl)^2 \exp.\left[-2\pi i(hu+kv+lw)\right]$

$$P(u,v,w) = \frac{1}{V^2}\sum_h\sum_k\sum_{l=-\infty}^{+\infty} F(hkl)^2 \cos 2\pi(hu+kv+lw) \qquad (8)$$

For the equatorial layer line, $l = 0$, and referring to the origin of the cell, equation 8 may be written,

$$P(x,y) = \frac{1}{V^2}\sum_h\sum_{k=-\infty}^{+\infty} F(hk0)^2 \cos 2\pi(hx+ky).$$

The Patterson series yields a type of density distribution which is periodic with the periodicity of the crystal, has maxima at the origin, and subsidiary maxima at vector distances from the origin equal to the vector distances between every pair of atoms in the crystal.

The summation of even a double series involves a considerable amount of numerical work, so it is desirable to reduce this as much as possible by utilizing one of the available shortened methods. Lipson and Beevers eased the work of summing these series by devising sets of cardboard strips upon which values of A sin $nh3^\circ$ and A cos $nh3^\circ$ are printed. The index values of h cover the range of from -30 to +30 in steps of unity. The amplitudes A range from -99 to +99 in steps of unity and from $\pm$ 100 to $\pm$ 900 in steps

of 100. n assumes values from 0 to 30 in steps of 1/30. In using these strips to perform the summation of the Patterson function, the $\cos 2\pi hx$ term of the Patterson series must be equivalent in value to $\cos nh3^{\circ}$ of the strips for every value of n. In order for this to be true x must vary in the same way as n. For example, if n assumes values of from 0 to 30/30, x will vary from 0 to 1, and the summation will have been conducted over one side of the unit cell. In order to facilitate the handling of the strips, n was divided by two and h doubled. This did not change the value of the strips, but made it necessary to sum over only the even integer values of h. In this case, however, n assumed values of from 0 to 15/30, and consequently, the summation occurred over 1/2 the cell edge. The same strips and techniques were used to carry out summations with respect to k. The results of the summation are given in Table 2.

REDUCTION OF DATA

The crystal was found to be monoclinic by analysis of the $\ell = 0,1,2$ reciprocal lattices. The origins of the first and second layer reciprocal lattices were not displaced thus indicating that the b_3 axis was perpendicular to the b_1, and b_2 axis and also parallel to the a_3 axis. The b_1, b_2 axes were unequal in length and contained an acute angle, β_{12}. When referred to real space this gives the a_1, a_2 axes containing an obtuse angle, α_{12}. The conditions for the monoclinic system are thus satisfied in that there are three unequal axes, one perpendicular to the plane of the other two, and the two coplanar axes containing an obtuse angle. The relation between components of a real and reciprocal space are (2):

Table 2. The results of the Fourier summation of the Patterson function.

y \ X	0	1/30	2/30	3/30	4/30	5/30	6/30	7/30	8/30	9/30	10/30	11/30	12/30	13/30	14/30	15/30
0	1787.	1414.	914.	806.	904.	874.	699.	591.	621.	655.	694.	661.	624.	624.	652.	723.
1/30	1548.	1253.	854.	755.	817.	849.	710.	600.	609.	637.	679.	650.	619.	623.	648.	701.
2/30	1019.	885.	693.	626.	673.	752.	704.	610.	584.	596.	635.	628.	610.	609.	630.	659.
3/30	512.	528.	506.	472.	493.	574.	616.	586.	554.	549.	584.	609.	603.	592.	606.	622.
4/30	278.	312.	356.	367.	365.	399.	482.	530.	524.	520.	548.	592.	593.	569.	567.	578.
5/30	207.	226.	279.	343.	346.	327.	397.	478.	495.	503.	521.	569.	590.	568.	538.	538.
6/30	234.	242.	282.	385.	411.	363.	400.	478.	502.	509.	529.	570.	593.	568.	530.	519.
7/30	384.	357.	372.	455.	493.	479.	487.	542.	561.	563.	594.	618.	618.	587.	562.	569.
8/30	532.	504.	482.	499.	542.	597.	588.	597.	606.	634.	655.	646.	610.	581.	579.	591.
9/30	693.	649.	598.	577.	647.	755.	706.	646.	642.	677.	731.	671.	610.	596.	609.	620.
10/30	851.	578.	658.	678.	794.	874.	760.	662.	647.	677.	726.	663.	613.	607.	624.	642.
11/30	964.	823.	679.	740.	819.	867.	716.	637.	623.	628.	666.	632.	616.	618.	630.	648.
12/30	964.	833.	680.	712	785	723.	602.	575.	626.	585.	601.	589.	615.	632.	627.	628.
13/30	781.	733.	652.	610.	594.	543.	499.	522.	530.	547.	548.	567.	611.	637.	616.	589.
14/30	530.	588.	601.	508.	436.	397.	446.	503.	496.	515.	545.	573.	610.	624.	601.	559.
15/30	406.	541.	572.	465.	380.	352.	431.	499.	483.	499.	540.	580.	611.	612.	595.	548.

$$v_a = \frac{a_3}{b_1 b_2 \sin \beta_{12}}$$

$$a_1 = \frac{b_2 \times b_3}{v_b}$$

$$a_2 = \frac{b_3 \times b_1}{v_b}$$

$$a_3 = \frac{b_1 \times b_2}{v_b}$$

$$\alpha_{31} = \alpha_{23} = 90^\circ$$

$$\alpha_{12} = 180^\circ - \beta_{12}$$

a_1, a_2, a_3 = unit cell axes in real space

$\alpha_{12}, \alpha_{13}, \alpha_{23}$, = axes angles in real space

b_1, b_2, b_3 = unit cell axes in reciprocal space

$\beta_{12}, \beta_{23}, \beta_{13}$ = axes angles in reciprocal space

v_a = unit cell volume

v_b = reciprocal unit cell volume

$v_a = 1/v_b$

The value of a_3 was computed from measurement of the rotation photograph. For an aligned crystal $a_3 = \frac{\ell \lambda}{\sin \beta}$.

From Plate VII:

$$\tan \beta = y/R$$

or

$$\beta = \tan^{-1} y/R$$

Therefore

$$a_3 = \frac{\ell \lambda}{\sin (\tan^{-1} y/R)}$$

Substituting in the proper value of ℓ and λ and the measured y/R gives the magnitude of a_3. The equatorial reciprocal lattice was measured with a calibrated steel rule to obtain the values of λb_1 and λb_2. A precision protractor was used to measure the angle β_{12}.

Substituting the measured quantities (b_1, b_2, a_3 and β_{12}) into the above relationships gives the unit cell dimensions and the unit cell volume.

$$a_1 = 12.617 \pm .012 A^\circ$$

$$a_2 = 8.748 \pm .044 A^\circ$$

$$a_3 = 7.169 \pm .007 A^\circ$$

$$\alpha_{12} = 111^{\circ}\ 11' \pm 5.5'$$

$$v_a = 737.8 \pm 4.4\ A^{03}$$

A knowledge of the number of molecules per unit cell is an important aid in determining to which one of the 13 possible monoclinic space groups the crystal belongs. The number of molecules per unit cell is

$$n = \frac{N v \rho}{A}$$

n = number of molecules per unit cell

ρ = density in grams per cc

N = number of molecules per mole

v = volume in cc per unit cell

A = number of grams per mole

Solving for the ratio ρ/n and substituting in the values for A, N, and v gives

$$\rho/n = 1.483 \pm .009 \qquad (9)$$

The density was determined by placing a known amount of the material into a calibrated pipette containing water and observing the change in height of the water column. The increase in column height caused by addition of one ml water to the pipette was noted, and the volume of cis material determined from the relation

$$\frac{\text{volume of cis}}{\text{1 cc water}} = \frac{\text{change in water column height by cis}}{\text{change in water column height by 1 ml water}}$$

This procedure along with the mass of the crystals used gives an experimental density of

$$\rho = 2.78 \pm 0.026\ \text{gms/cc}$$

Since the solubility of the cis in water was not known, and since some of the material surely went into solution, the measured value of the density is probably somewhat lower than the true density. Substituting the value of ρ

into equation 9 and solving for n gives a value of two molecules per unit cell. The value n = 2 was then substituted into equation (9) and the x-ray determined density value found was equal to 2.966 ± 0.018 gms/cc.

The cis derivative, since it is monoclinic, may belong to any one of 13 possible space groups. The systematic absence of spectra provides the data for the deduction of the space group. In order to determine which spectra was not present the $\ell = 1$ and $\ell = 2$ layer line reciprocal lattices were plotted and each reflection indexed. Tables listing the space groups and conditions for their existance were consulted and by the process of elimination it was found that the cis belongs to either one of two groups (5). The two groups as given by their Schoenflies symbols are:

1. C_s^2 with the center of each molecule at x, y, z and x, $\bar{y}$, $\frac{1}{2}$ + z.

2. C_2^4 with the center at $\frac{1}{2}$, y, $\frac{1}{4}$ and $\frac{1}{2}$, $\bar{y}$, 3/4 or o, y, $\frac{1}{4}$ and o, $\bar{y}$, 3/4.

The Patterson functions exhibits peaks at vector distances from the origin equal to vector distances between pairs of maxima in the electron density. The height of each peak is proportional to the product of the scattering powers of the two atoms concerned (3). The $F(hkl)^2$ synthesis used gives a large peak at the origin, which expresses the fact that any atom is at zero distance from itself.

The interpretation of the Patterson series for complex structures is difficult. This is due to the fact that for unit cells containing many atoms, some of the vectors are very likely to lie close together so that the individual peaks are not resolved. Also, the chances of overlapping are great. Therefore, in order to completely fix the atomic distribution in space, it may be necessary to obtain a density map projected along one of

the other two coordinate axis. The correctness of the positions can then be checked from the projection along the third axis.

A reproduction of the electron density contour map produced by the synthesis of all the hk0 values is shown in Plate IX. The x and y coordinate and the magnitudes of the eight resolved peaks are given in Table 3. Attempts to determine the actual positions of the mercury atoms have not been successful at this time.

Table 3. Indices and magnitudes of the peaks on the Patterson plot.

No.	Maximum	x coordinates	y coordinates
0	1787	0	0
1	1032	0	31/80
2	878	63/375	81/240
3	735	10/30	29/96
4	640	13/30	209/480
5	650	15/30	87/240
6	725	15/30	1/240
7	694	10/30	0
8	908	101/750	0

CONCLUSION

The crystal was found to belong to the monoclinic system and be in either the C_s^2 or C_{2h}^4 space group. The unit cell dimensions were computed to be:

$$a_1 = 12.617 \pm .012A^\circ$$

$$a_2 = 8.748 \pm .044A^\circ$$

$$a_3 = 7.169 \pm .007A^\circ$$

EXPLANATION OF PLATE IX

A reproduction of the electron density contour map resulting from the Patterson analysis.

PLATE IX

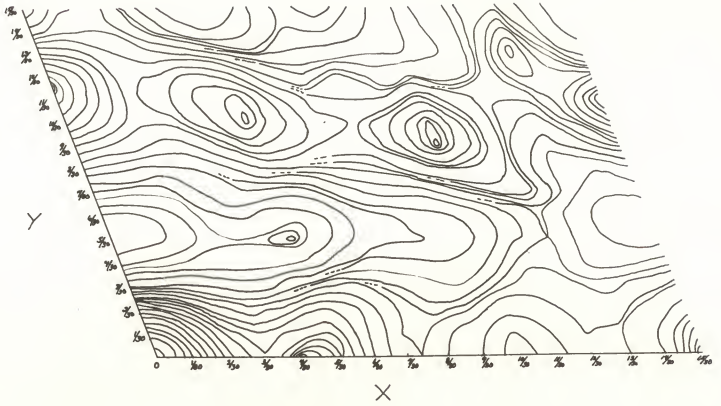

$$\alpha_{12} = 111^{\circ}\ 11' \pm 5.5'$$

$$v_a = 737.8 \pm 4.4 A^3$$

The cis derivative contains two molecules per unit cell, and has an x-ray determined density of 2.966 ± .018 gms/cc. The contour map plotted from information obtained from the Patterson analysis gave vector relations between points of high electron density. The interpretation of the map to give the actual atomic distribution has not been accomplished at this time.

FUTURE STUDIES

The information that can be obtained from a two dimensional Patterson synthesis usually depends upon the complexity of the molecule being studied. In the F_{hk0}^2 projection, the vector corresponding to a given interatomic distance is always drawn from the origin, no matter where the two atoms may lie in the true projection. If there are several equal and parallel interatomic distances in the true projection, all give the same peak on the contour map. The plot may also be further complicated by overlapping and unresolved maxima. One method of overcoming this deficiency is to obtain a density map projected along one of the other two coordinate axis. This should give sufficient information to fix the position of the heavy atoms. This procedure could not be followed unless there were some means of rotating the crystal on its mount so that proper alignment could be obtained.

The maxima in the F_{hk0}^2 distribution are rather diffuse because the coefficients F_{hk0}^2 of the series diminish rapidly. Patterson devised a way to systematically decrease the rate at which the coefficients fall off, thus sharpening the maxima in the distribution given by the series. Patterson

suggests using F(hk) $/\bar{f}$ in the coefficients instead of F(hk) where;

$$\bar{f} = \sum_m f_m / F(00) \qquad f_m = \text{scattering factor of } m^{th} \text{ atom.}$$

the summation being over all atoms in the unit cell. The general effect of this is to produce a scattering factor corresponding more closely to one due to point atoms, and to sharpen the maxima in the resulting distribution.

Probably the most common procedure for fixing the positions of the atoms in a unit cell is to carry out at least a two-dimensional F_{hk0}^2 synthesis to see if it yields any clear information on the positions of some of the atoms or the general form or orientation of the molecule. If it does yield such information, this may be sufficient to settle the signs of some of the F_{hk0}'s, which are then used for a regular Fourier electron density analysis. This first electron density map should indicate approximate positions for the lighter atoms thus giving information for the recalculating of the doubtful signs. A second, third, etc. F_{hk0} synthesis can be performed until the desired refinement is reached.

ACKNOWLEDGMENT

The excellent advice, encouragement, and help given by Dr. R. D.Dragsdorf throughout this research are gratefully acknowledged. Appreciation is also expressed to Dr. S. E. Whitcomb for his much appreciated moral support, and to the members of the faculty for their understanding of the personal problems encountered.

REFERENCES

1. Bijvoet, J. M.
X-ray Analysis of Crystals. New York: Interscience Publishers Inc. 1951. Chapt. V, VI: Appendix I, V, VI.

2. Buerger, M. J.
X-ray Crystallography. New York: John Wiley and Sons. 1953. Chapt. V, VI, VIII, XI, XII, XIII, XXII.

3. Bunn, C. W.
Chemical Crystallography. London: Oxford University Press. 1946. Chapt. IX.

4. Dragsdorf, R. D.
Crystal Alignment on the Weissenberg Goniometer. Acta Cryst. 6:220 (1953).

5. Henry, Norman F. M. and K. Lonsdale.
International Tables for X-ray Crystallography. Birmingham: Kynoch Press. 1952.

6. James, R. W.
The Optical Principles of the Diffraction of X-rays. London: G. Bell and Sons Ltd. 1948. Chapt. II, III, VII. Appendix II.

7. Sproull, W. T.
X-rays in Practice. New York: McGraw-Hill Book Co. Inc. 1946. Chapt. XV, XVII.

8. Whitehead, E. V., R. A. Dean, and F. A. Fidler.
The Preparation and Physical Properties of Sulfur Compounds Related to Petroleum. Jour. Am. Chem. Soc. 73:3632. 1951.

X-RAY ANALYSIS OF THE CIS FORM OF 2.5 DIMETHYLTHIACYCLOPENTANE

by

GEORGE RAY GALLAGHER

A. B., Kansas State Teachers College, Emporia, 1953

AN ABSTRACT OF A THESIS

submitted in partial fulfillment of the

requirements for the degree

MASTER OF SCIENCE

Department of Physics

KANSAS STATE COLLEGE
OF AGRICULTURE AND APPLIED SCIENCE

1955

The 2,5 Dimethylthiacyclopentane molecule occurs in the cis and trans forms. The cis form of the mercuric chloride complex contains two mercuric chloride groups both presumed to be positioned on the same side of the ring. The trans isomer has only one mercuric chloride group.

The object of this study was to determine the crystal structure and, if possible, the relationships of the mercury atoms in the cis form of the mercuric chloride complex of the 2,5 Dimethylthiacyclopentane molecule. The x-ray diffraction method using moving film techniques was the means chosen to study the problem.

The Weissenberg camera was used to obtain a rotation photograph and also normal beam Weissenberg photographs of the $\ell = 0$, 1 and 2 layer lines. The a_3 axial length was determined for the layer separation on the rotation pattern. Then, using data taken from the $\ell = 0$ layer line, the reciprocal lattice was constructed, measurement of which yielded the lengths of the reciprocal space parameters b_1, b_2 and the magnitude of their included angle, β_{12}. A calibration intensity strip was made in order to obtain the relative intensity, I, of each diffraction spot. The relative crystal structure factors squared, $F(hkl)^2$, for each reflection was calculated, using the relative intensity and the Lorenz-Polarization term, from the expression, $I \propto (L.P.)\, F(hkl)^2$. A knowledge of the $F(hkl)^2$ values made it possible to use the Patterson analysis to obtain information about interatomic distances. The Patterson series when summed by Fourier methods yields a type of density distribution which is periodic with the periodicity of the crystal. The summation provided data for the construction of a contour map which showed peaks at vector distances from the origin equal to vector distances between pairs of maxima in the electron density.

Analysis of the $\ell = 0, 1, 2$ reciprocal lattices placed the crystal in the monoclinic system. The unit cell axes and included angle in real space, a_1, a_2 and α_{12}, were computed using equations relating reciprocal to real space. The cis form was found to contain two molecules per unit cell, and have a density of 2.966 ± 0.018 gms/cc. The 13 possible monoclinic space groups to which the crystal could belong were reduced to two. These groups as given by their Schoenflies symbols are C_s^2 and C_{2h}^4.